

# Comptonization and the Spectra of Accretion-Powered X-Ray Pulsars

Michael T. Wolff\*, Peter A. Becker<sup>†</sup> and Kenneth D. Wolfram<sup>†,\*</sup>

*\*Space Science Division, Naval Research Laboratory, Washington, DC 20375*

*†Center for Earth Observing and Space Research, George Mason University, Fairfax, VA 22030-4444*

**Abstract.** Accretion-powered X-ray pulsars are among the most luminous X-ray sources in the Galaxy. However, despite decades of theoretical and observational work since their discovery, no satisfactory model for the formation of the observed X-ray spectra has emerged. In this paper, we report on a self-consistent calculation of the spectrum emerging from a pulsar accretion column that includes an explicit treatment of the bulk and thermal Comptonization occurring in the radiation-dominated shocks that form in the accretion flows. Using a rigorous eigenfunction expansion method, we obtain a closed-form expression for the Green's function describing the upscattering of monochromatic radiation injected into the column. The Green's function is convolved with bremsstrahlung, cyclotron, and blackbody source terms to calculate the emergent photon spectrum. We show that energization of photons in the shock naturally produces an X-ray spectrum with a relatively flat continuum and a high-energy exponential cutoff. Finally, we demonstrate that our model yields good agreement with the spectra of the bright pulsar Her X-1 and the low luminosity X Per.

**Keywords:** Neutron stars, Accretion, X-Rays, Comptonization, Radiation-dominated shocks

**PACS:** 95.30.Jx, 97.60.Gb, 97.80.Jp, 98.35.Mp

## INTRODUCTION

Accreting X-ray pulsars were discovered in the late 1960s by rocket flights from White Sands in New Mexico [1, 2]. Since that time the number of known X-ray pulsars of all types has grown to over 100. The prevailing model for accreting X-ray pulsars consists of a neutron star orbiting a normal stellar companion that is losing matter via either Roche lobe overflow or a stellar wind. Accreting X-ray pulsar spectra are characterized by a power-law dependence on energy in the range above  $\sim 3$  keV with a quasi-exponential cutoff at higher energies, typically near 20–40 keV. For example, see the X-ray spectrum of 4U11626-67 reported by Orlandini [3], or the multiple source spectra reported by Coburn et al. [4]. Cyclotron features have also been observed in many sources [4].

Comptonization is known to play an important role in the X-ray pulsar spectral formation process. This is a general result, based on the overall spectral shape (a power-law) and the fact that Comptonization tends to result in a power-law dependence with energy in many accreting compact object sources. The usual method of characterizing accreting X-ray pulsar spectra is to fit the broad-band X-ray spectra using a number of ad-hoc functions such as power-laws, Gaussian emission line features, Gaussian or Lorentzian absorption features, and various types of quasi-exponential high-energy cutoffs. However, most of these functional forms have little physical motivation beyond the fact that they “look like the spectra” and they are easy to incorporate into spectral fitting pro-

grams (e.g., XSPEC). The real physical parameters of the source (e.g., accretion rate, accretion region size, shock height, plasma temperature, etc.) are not directly connected with the ad hoc parameters and are in fact much harder to determine.

Three principal models have been put forward to explain the energy spectra of accreting X-ray pulsars: the gas-mediated collisionless shock model [5]; the Coulomb collisional stopping model [6, 7, 8]; and the radiation-dominated flow model [9, 10]. The collisionless shock model and the Coulomb collisional model can only be applied in the case of low-luminosity accretion onto neutron stars. In such models, the effects of radiation pressure are assumed to be small, and the flow impinges directly onto the neutron star surface (in the absence of other effects; see below). These models tend to produce pencil-beamed emission patterns because the radiation escapes primarily through the top of the neutron star atmosphere. In high-luminosity pulsars, the dynamical structure is expected to be dominated by the effects of radiation pressure, which decelerates the gas to rest at the stellar surface. The radiation-dominated inflow models of Davidson [9] and Arons et al. [10] attempt to describe the flow dynamics across a broad range of X-ray pulsar luminosities, all the way up to the Eddington limit.

Neither the collisionless shock model nor the Coulomb collisional model have demonstrated good agreement with actual X-ray pulsar spectra. Mészáros and Nagel [11] compared the spectrum of Her X-1 with results obtained using the Coulomb collisional model. The observed Her X-1 spectrum was not well fit by the calculated spectra. Furthermore, the applicability of the Coulomb collisional model to Her X-1 is questionable because the source luminosity is believed to be close to the Eddington limit ( $L_x \sim 2.2 \times 10^{37}$  ergs s<sup>-1</sup> at 5 kpc), implying that radiation pressure is important [12, 13]. For further discussion of Coulomb collisional stopping models see Harding and Lai [14] and references therein.

Insight into the photon transport in the accretion column can be gained by estimating the optical depth to electron scattering in the magnetic field direction,  $\tau_{\parallel}$ , and the scattering optical depth across the accretion column,  $\tau_{\perp}$ . Assuming Thomson scattering and a free-fall velocity profile, we can express these quantities in cgs units using [see 15]

$$\tau_{\parallel} \sim 20 \left( \frac{L_x}{10^{37}} \right) \left( \frac{R_{\text{ns}}}{10^6} \right)^{5/2} \left( \frac{M_{\text{ns}}}{1.4 M_{\odot}} \right)^{-3/2} \left( \frac{r_0}{10^5} \right)^{-2}, \quad (1)$$

and

$$\tau_{\perp} \sim 3 \left( \frac{L_x}{10^{37}} \right) \left( \frac{R_{\text{ns}}}{10^6} \right)^{3/2} \left( \frac{M_{\text{ns}}}{1.4 M_{\odot}} \right)^{-3/2} \left( \frac{r_0}{10^5} \right)^{-1}, \quad (2)$$

where  $L_x$  is the accretion luminosity,  $M_{\text{ns}}$  and  $R_{\text{ns}}$  are the neutron star mass and radius, respectively, and  $r_0$  is the radius of the accretion region on the neutron star surface. Based on the modeling described below, we find that  $\tau_{\parallel} \sim 6.5 \times 10^{-2}$  and  $\tau_{\perp} \sim 4.2 \times 10^{-3}$  for X Per. Conversely, in the Her X-1 case we obtain  $\tau_{\parallel} \sim 2.1 \times 10^4$  and  $\tau_{\perp} \sim 1.4 \times 10^2$ . Hence photons will scatter many more times while escaping from the accretion flow in Her X-1 than in X Per. This is a general result that applies to all high-luminosity X-ray pulsars such as Her X-1 because of the larger accretion rates compared with the low-luminosity, steep spectrum sources such as X Per.

## A RADIATION-DOMINATED SHOCK MODEL FOR X-RAY PULSAR SPECTRA

Adopting a cylindrical, plane-parallel geometry for the accretion column with the magnetic field in the  $z$ -direction, the Green's function  $f_G(z_0, z, \varepsilon_0, \varepsilon)$  satisfies the modified [16] steady-state transport equation [see, e.g., 17, 18]

$$\begin{aligned} v \frac{\partial f_G}{\partial z} &= \frac{dv}{dz} \frac{\varepsilon}{3} \frac{\partial f_G}{\partial \varepsilon} + \frac{\partial}{\partial z} \left( \frac{c}{3n_e \sigma_{\parallel}} \frac{\partial f_G}{\partial z} \right) - \frac{f_G}{t_{\text{esc}}} + \frac{n_e \bar{\sigma} c}{m_e c^2} \frac{1}{\varepsilon^2} \frac{\partial}{\partial \varepsilon} \left[ \varepsilon^4 \left( f_G + kT_e \frac{\partial f_G}{\partial \varepsilon} \right) \right] \\ &+ \frac{\dot{N}_0 \delta(\varepsilon - \varepsilon_0) \delta(z - z_0)}{\pi r_0^2 \varepsilon_0^2}, \end{aligned} \quad (3)$$

where  $z$  is the altitude above the stellar surface,  $v < 0$  is the inflow velocity,  $\dot{N}_0$  is the rate of injection of seed photons with energy  $\varepsilon_0$  at location  $z_0$ ,  $t_{\text{esc}}$  represents the mean time photons spend in the plasma before diffusing through the walls of the column,  $\sigma_{\parallel}$  is the electron scattering cross section for photons propagating parallel to the magnetic field,  $\bar{\sigma}$  is the angle-averaged cross section, and  $T_e$ ,  $n_e$ , and  $m_e$  denote the electron temperature, number density, and mass, respectively. The mean escape time is computed using  $t_{\text{esc}} = r_0/w_{\perp}$ , where  $w_{\perp} = c/\tau_{\perp}$  is the diffusion velocity perpendicular to the  $z$ -axis,  $\tau_{\perp} = n_e \sigma_{\perp} r_0$  is the electron scattering optical thickness across the column, and  $\sigma_{\perp}$  denotes the electron scattering cross section for photons propagating perpendicular to the magnetic field. The solution for the Green's function  $f_G(z_0, z, \varepsilon_0, \varepsilon)$  is obtained by deriving eigenvalues and associated eigenfunctions based on the set of spatial and energetic boundary conditions for the problem [see 17]. We define a source function  $Q$  such that  $\varepsilon^2 Q(z, \varepsilon) d\varepsilon dz$  gives the number of seed photons injected per unit time in the altitude range  $z$  to  $z + dz$  and energy range  $\varepsilon$  to  $\varepsilon + d\varepsilon$ . Once we have the analytical solution for the Green's function, the particular solution corresponding to bremsstrahlung, cyclotron, or blackbody source distributions can be obtained via the integral convolution

$$f(z, \varepsilon) = \int_0^{\infty} \int_0^{\infty} \frac{f_G(z_0, z, \varepsilon_0, \varepsilon)}{\dot{N}_0} \varepsilon_0^2 Q(z_0, \varepsilon_0) d\varepsilon_0 dz_0. \quad (4)$$

In the models described here, the effects of bulk and thermal Comptonization are treated explicitly using the transport terms in equation (3). The importance of dynamical (bulk) versus thermal Comptonization depends on the parameter  $\delta \equiv (\alpha \sigma_{\parallel} / 3\bar{\sigma})(m_e c^2 / kT_e)$ , where  $\alpha \sim 0.3 - 0.5$  describes the velocity variation as a function of the optical depth above the stellar surface. It can be shown that  $\delta$  is essentially the ratio of the ‘‘y-parameters’’ for bulk and thermal Comptonization. When  $\delta$  is of order unity, the two processes are comparable, and when  $\delta \gg 1$ , the bulk process dominates. Another important spectral formation parameter is  $\xi \equiv (\pi r_0 m_p c) / (\dot{M} \sqrt{\sigma_{\parallel} \sigma_{\perp}})$ , where  $\dot{M}$  denotes the accretion rate and  $m_p$  is the proton mass. We find that  $\xi$  is roughly equal to the ratio of the dynamical (accretion) timescale divided by the timescale for the photons to diffuse through the column walls. The condition  $\xi \sim 1$  must be satisfied in order to ensure that radiation pressure decelerates the gas to rest at the stellar surface.

## RESULTS FOR X-RAY PULSAR SPECTRA

Using our model we can compute the theoretical spectrum emitted from an X-ray pulsar accretion column due to Comptonized bremsstrahlung, cyclotron, and blackbody seed photons. The theoretical phase-averaged photon count rate spectrum,  $F_\varepsilon(\varepsilon)$ , is given by

$$F_\varepsilon(\varepsilon) \equiv \frac{\Phi_\varepsilon(\varepsilon)}{4\pi D^2}, \quad \Phi_\varepsilon(\varepsilon) \equiv \int_0^\infty \frac{\pi r_0^2 \varepsilon^2}{t_{\text{esc}}(z)} f(z, \varepsilon) dz, \quad (5)$$

where  $\Phi_\varepsilon(\varepsilon)$  represents the vertically-integrated escaping photon number spectrum,  $f(z, \varepsilon)$  is computed using equation (4), and  $D$  is the distance to the source. As a check on our results for the spectra, we confirm that the number of photons escaping from the column per unit time is exactly equal to the number injected, as required by our steady-state scenario.

In Figure 1 we plot the theoretical count-rate spectrum  $F_\varepsilon(\varepsilon)$  evaluated using equation (5) along with the deconvolved, phase-averaged *BeppoSAX* spectrum of Her X-1 reported by dal Fiume et al. [19]. The theoretical parameters in this case are  $\alpha = 0.40$ ,  $\xi = 1.45$ ,  $\sigma_\perp = \sigma_T$ ,  $\delta = 1.8$ ,  $B = 3.80 \times 10^{12}$  G,  $\dot{M} = 1.11 \times 10^{17}$  g s<sup>-1</sup>,  $r_0 = 44$  m,  $T_e = 6.25 \times 10^7$  K, and  $T_{\text{th}} = 5.68 \times 10^7$  K, where  $\sigma_T$  denotes the Thomson cross section and  $T_{\text{th}}$  is the thermal mound temperature. We assume a source distance of  $D = 5$  kpc. In Figure 1 results are plotted for the total spectrum, as well as for the individual contributions to the observed flux due to the Comptonization of cyclotron, blackbody, and bremsstrahlung seed photons. The theoretical spectrum in Figure 1 also includes an iron emission line.

The general shape of the theoretical spectrum agrees with the observations for Her X-1 quite well, including both the quasi-exponential cutoff energy and the power-law slope. In the case of Her X-1, reprocessed (Comptonized) blackbody emission from the thermal mound makes a negligible contribution to the spectrum because the radius of the accretion column is relatively small. Due to the high temperature of the post-shock plasma, the reprocessed cyclotron emission is overwhelmed by reprocessed bremsstrahlung emission, which dominates the observed spectrum.

The second source, 4U 0352+30 (X Per), is a low-luminosity ( $L_x \sim 10^{34}$  ergs s<sup>-1</sup>) X-ray pulsar with a relatively steep spectrum. This pulsar was discussed by Becker and Wolff [20, 21] using a pure-bulk Comptonization model, and it therefore represents an interesting test for the thermal+bulk model developed by Becker and Wolff [17] and described in this paper. In Figure 2 we compare the theoretical spectrum with archival *RXTE* data taken in July 1998 and reported by Delgado-Martí et al. [22]. The theory parameters in this case are  $\alpha = 0.51$ ,  $\xi = 1.85$ ,  $\sigma_\perp = \sigma_T$ ,  $\delta = 10.9$ ,  $B = 3.30 \times 10^{12}$  G,  $\dot{M} = 3.23 \times 10^{13}$  g s<sup>-1</sup>,  $r_0 = 430$  m,  $T_e = 4.00 \times 10^7$  K,  $T_{\text{th}} = 9.00 \times 10^6$  K, and  $D = 0.35$  kpc. The distance and magnetic field values are from Negueruela [23] and Coburn et al. [24], respectively. In contrast to the case of Her X-1, our model shows that the spectrum of X Per is dominated by Comptonized *blackbody* emission, which is due to the order of magnitude increase in the radius of the accretion column. Reprocessed cyclotron and bremsstrahlung radiation make a negligible contribution to the observed spectrum for this source. The spectral results obtained here using the thermal+bulk Comptonization model are nearly identical to those obtained by Becker and Wolff

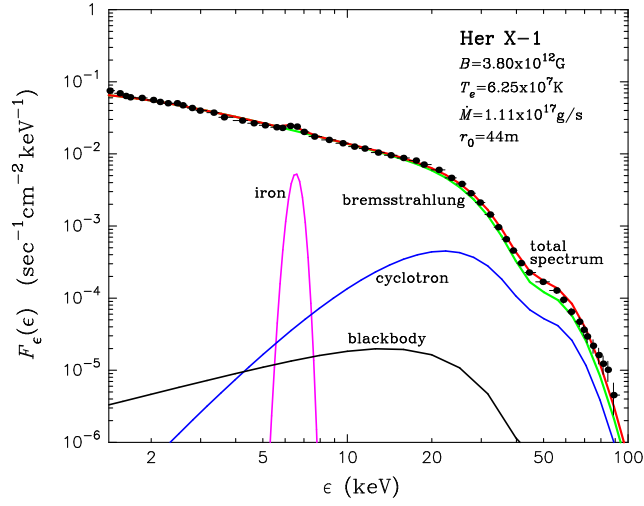


**FIGURE 1.** Theoretical spectrum of Her X-1 based on our radiation-dominated, radiative shock model (eq. [5]), compared with the data reported by dal Fiume et al. [19].

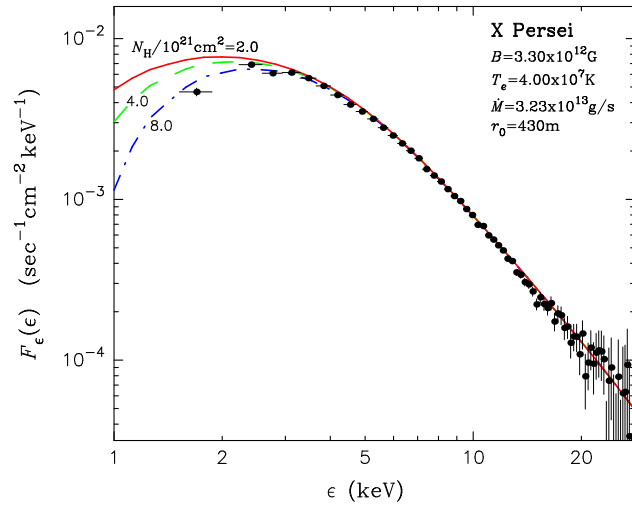


**FIGURE 2.** Theoretical spectrum of X Per based on our radiation-dominated, radiative shock model (eq. [5]), compared with the data reported by Delgado-Martí et al. [22]. Various amounts of interstellar absorption have been included as indicated.

[21, 20], which is consistent with the fact that the spectral formation in this source is dominated by bulk Comptonization, as indicated by the large value of  $\delta$ .

## CONCLUSIONS

We have developed a new analytical model describing the spectral formation process in accretion-powered X-ray pulsars. The model includes a rigorous treatment of both the bulk and thermal Comptonization occurring in the radiation-dominated, radiative

shock. These two types of Comptonization influence different regions of the radiation distribution and can explain a wide range of accretion-powered X-ray pulsar spectra. We have shown that the theoretical spectra produced by our model in luminous sources such as Her X-1 are dominated by Comptonized bremsstrahlung emission, not Comptonized cyclotron emission as was previously conjectured. On the other hand, we find that the spectra of low-luminosity sources such as X Per are dominated by Comptonized blackbody radiation. Our new Comptonization model provides greatly improved fits to the observed spectral data when compared with the gas-mediated collisionless shock or Coulomb collisional models. Furthermore, the X-ray spectra produced by our model can be evaluated using a single-pass, closed-form algorithm that does not require numerical iteration. Our model should therefore be suitable for incorporation into the XSPEC spectral modeling environment and we expect to complete that work in the near future.

## ACKNOWLEDGMENTS

The authors wish to thank Drs. Lev Titarchuk, Kent Wood, and Jean Swank for useful discussions. This research was funded by NASA and the Office of Naval Research.

## REFERENCES

1. Chodil, G., Mark, H., Rodrigues, R., Seward, F., Swift, C. D., Hiltner, W. A., Wallerstein, G., and Mannery, E. J., *Phys. Rev. Lett.*, **19**, 681 (1967).
2. Giacconi, R., Gursky, H., Kellogg, E., Schreier, E., and Tananbaum, H., *ApJ*, **167**, L67+ (1971).
3. Orlandini, M., pp. preprint [astro-ph/0510267] (2005), to appear in the Proceedings of COSPAR Colloquium 'Spectra & Timing of Compact X-ray Binaries,' January 17-20, 2005, Mumbai, India.
4. Coburn, W., Heindl, W. A., Rothschild, R. E., Gruber, D. E., Kreykenbohm, I., Wilms, J., Kretschmar, P., and Staubert, R., *ApJ*, **580**, 394 (2002).
5. Langer, S. H., and Rappaport, S., *ApJ*, **257**, 733 (1982).
6. Mészáros, P., Harding, A. K., Kirk, J. G., and Galloway, D. J., *ApJ*, **266**, L33 (1983).
7. Miller, G. S., Salpeter, E. E., and Wasserman, I., *ApJ*, **314**, 215 (1987).
8. Miller, G., Wasserman, I., and Salpeter, E. E., *ApJ*, **346**, 405 (1989).
9. Davidson, K., *Nat. Phys. Sci.*, **246**, 1 (1973).
10. Arons, J., Klein, R. I., and Lea, S. M., *ApJ*, **312**, 666 (1987).
11. Mészáros, P., and Nagel, W., *ApJ*, **298**, 147 (1985).
12. White, N. E., Swank, J. H., and Holt, S. S., *ApJ*, **270**, 711 (1983).
13. Dal Fiume, D., Orlandini, M., Cusumano, G., Del Sordo, S., Feroci, M., Frontera, F., Oosterbroek, T., Palazzi, E., Parmar, A. N., Santangelo, A., and Segreto, A., *A&A*, **329**, L41 (1998).
14. Harding, A. K., and Lai, D., *Reports of Progress in Physics*, **69**, 2631 (2006).
15. Imamura, J. N., and Durisen, R. H., *ApJ*, **268**, 291 (1983).
16. Kompaneets, A. S., *Sov. Phys.-JETP*, **4**, 730 (1957).
17. Becker, P. A., and Wolff, M. T., *ApJ*, **in press**, astro-ph/0609035 (2006).
18. Becker, P. A., and Begelman, M. C., *ApJ*, **310**, 534 (1986).
19. dal Fiume, D., Orlandini, M., Cusumano, G., del Sordo, S., Feroci, M., Frontera, F., Oosterbroek, T., Palazzi, E., Parmar, A. N., Santangelo, A., and Segreto, A., *A&A*, **329**, L41 (1998).
20. Becker, P. A., and Wolff, M. T., *ApJ*, **621**, L45 (2005).
21. Becker, P. A., and Wolff, M. T., *ApJ*, **630**, 465 (2005).
22. Delgado-Martí, H., Levine, A. L., Pfahl, E., and Rappaport, S. A., *ApJ*, **546**, 455 (2001).
23. Negueruela, I., *A&A*, **338**, 505 (1998).
24. Coburn, W., Heindl, W. A., Gruber, D. E., Rothschild, R. E., Staubert, R., Wilms, J., and Kreykenbohm, I., *ApJ*, **552**, 738 (2001).